

From Mineralogy to Mechanical Properties: integrating core data and rock physics simulations for stiffness tensor estimation in Vaca Muerta organic-rich mudrock

Juan E. Santos, School of Earth Sciences and Engineering, Hohai University, Universidad de Buenos Aires, Facultad de Ingeniería, Instituto del Gas y del Petróleo, Department of Mathematics, Purdue University, A. Sanchez Camus, Facultad de Ciencias Astronómicas y Geofísicas, Universidad Nacional de La Plata, Solaer Ingeniería S.A., Gabriela B. Savioli, Universidad de Buenos Aires, Facultad de Ingeniería, Instituto del Gas y del Petróleo, Patricia M. Gauzellino, Facultad de Ciencias Astronómicas y Geofísicas, Universidad Nacional de La Plata, Jing Ba *, School of Earth Sciences and Engineering, Hohai University

SUMMARY

From a mechanical perspective, organic mudrocks are viscoelastic media whose anisotropy can be accurately represented using a vertical transverse isotropy (VTI) model. These reservoirs exhibit ultra-low permeability, typically in the range of nano to microdarcies, and possess a complex pore structure. Such characteristics, along with different oil, gas and water fluids saturations, significantly impact the hydraulic properties and mechanical behavior of the reservoir during production. This study introduces a practical methodology to estimate the stiffness tensor of dry rock using theoretical models of rock physics, incorporating mechanical, mineralogical, and petrophysical data from a core extracted from the lower section of the Vaca Muerta Formation (VMF), located in the Neuquén Basin, Argentina. This core was extracted from a block located in the maximum oil generation window of the Vaca Muerta formation at a depth of 3100 m. After determining the dry-rock stiffness tensor, the proposed methodology enables to analyze the effects caused by fluid saturation and seismic source frequencies, ranging from laboratory experiments and well logging to field seismic studies. Numerical results exhibit excellent agreement with laboratory phase velocities measured at 1 MHz, with errors below 5 %. The procedure is then validated as an effective tool for evaluating critical phenomena such as attenuation and dispersion caused by wave-induced fluid flow (WIFF). Once the model parameters have been calibrated, the stiffness tensor can be extrapolated to other areas within the block using only mineralogical and petrophysical information (porosity and permeability). This significantly simplifies the geomechanical and seismic characterization of unconventional reservoirs.

INTRODUCTION

The Vaca Muerta formation consists of a sequence of very thin layers which at long wavelengths compared with the average layer thickness. It behaves as a transversely isotropic anisotropy with a vertical axis - VTI (Sosa Massaro et al., 2018), although it may change its elastic symmetry due to the presence of fractures.

These type of formations were studied using different approaches.

White et al. (1975) obtained the complex and frequency-dependent P-wave stiffness associated with the symmetry axis of thin poroelastic layers.

Backus (1962) obtained the average elasticity constants in the case when the single layers are transversely isotropic with the symmetry axis perpendicular to the layering plane.

Gelinsky and Shapiro (1997) determined the relaxed and unrelaxed stiffnesses of the equivalent poro-viscoelastic medium to a periodic sequence of finely layered horizontally homogeneous material, while Krzikalla and Müller (2011) combined the two previous models to determine the five stiffnesses of the equivalent TIV medium.

The objective of this study is to verify that by knowing the mineralogy and applying these theoretical models of rock physics it is feasible to obtain accurate estimates the elastic tensor coefficients p_{ij} and their associate phase velocities.

THEORY FOR VTI MEDIA

A VTI medium is characterized by five independent elastic moduli $c_{11}, c_{13}, c_{33}, c_{55}, c_{66}$. In this case, the stress-strain relationship in Voigt notation is given by Tsvankin (2001),

$$\begin{bmatrix} \sigma_{11} \\ \sigma_{22} \\ \sigma_{33} \\ \sigma_{23} \\ \sigma_{31} \\ \sigma_{12} \end{bmatrix} = \begin{bmatrix} c_{11} & c_{12} & c_{13} & 0 & 0 & 0 \\ c_{12} & c_{11} & c_{13} & 0 & 0 & 0 \\ c_{13} & c_{13} & c_{33} & 0 & 0 & 0 \\ 0 & 0 & 0 & c_{55} & 0 & 0 \\ 0 & 0 & 0 & 0 & c_{55} & 0 \\ 0 & 0 & 0 & 0 & 0 & c_{66} \end{bmatrix} \cdot \begin{bmatrix} \epsilon_{11} \\ \epsilon_{22} \\ \epsilon_{33} \\ 2\epsilon_{23} \\ 2\epsilon_{31} \\ 2\epsilon_{12} \end{bmatrix} \quad (1)$$

with the vectors σ and ϵ being the stress and the strain, respectively, and $c_{12} = c_{11} - 2c_{66}$.

Attenuation and dispersion of the material can be represented through an equivalent viscoelastic medium, characterized by complex and frequency dependent stiffness p_{ij} , with the imaginary part representing attenuation. Therefore, with $\tilde{\sigma}$ and $\tilde{\epsilon}$ denote the stress and strain of the equivalent viscoelastic VTI medium we have the relations

$$\begin{bmatrix} \tilde{\sigma}_{11} \\ \tilde{\sigma}_{22} \\ \tilde{\sigma}_{33} \\ \tilde{\sigma}_{23} \\ \tilde{\sigma}_{31} \\ \tilde{\sigma}_{12} \end{bmatrix} = \begin{bmatrix} p_{11} & p_{12} & p_{13} & 0 & 0 & 0 \\ p_{12} & p_{11} & p_{13} & 0 & 0 & 0 \\ p_{13} & p_{13} & p_{33} & 0 & 0 & 0 \\ 0 & 0 & 0 & p_{55} & 0 & 0 \\ 0 & 0 & 0 & 0 & p_{55} & 0 \\ 0 & 0 & 0 & 0 & 0 & p_{66} \end{bmatrix} \cdot \begin{bmatrix} \tilde{\epsilon}_{11} \\ \tilde{\epsilon}_{22} \\ \tilde{\epsilon}_{33} \\ 2\tilde{\epsilon}_{23} \\ 2\tilde{\epsilon}_{31} \\ 2\tilde{\epsilon}_{12} \end{bmatrix} \quad (2)$$

where $p_{12} = p_{11} - 2p_{66}$.

White et al. (1975) and Carcione and Picotti (2006) described the equivalent viscoelastic medium of a periodic sequence of

From Mineralogy to Mechanical Properties using core data and rock physics for stiffness estimation in VMF

alternating thin horizontally homogeneous layers of thickness d_1 and d_2 , with symmetry axes normal to the layering plane. Their theory gives the complex and frequency dependent stiffness $p_{33}(\omega)$, as:

$$p_{33}(\omega) = \left[\frac{1}{c_{33}} + \frac{2(r_2 - r_1)^2}{i\omega(d_1 + d_2)(I_1 + I_2)} \right]^{-1}, \quad (3)$$

where

$$r = \frac{\alpha M}{E_G}, I = \frac{\eta}{\kappa a} \coth\left(\frac{ad}{2}\right), a = \sqrt{\frac{i\omega\eta E_G}{\kappa M E_m}} \quad (4)$$

for each single layer. In Eq.(4), $\alpha = 1 - \frac{K_m}{K_s}$, $E_G = E_m + \alpha^2 M$,

$E_m = K_m + \frac{4}{3}\mu$, $M = \left[\frac{\alpha - \phi}{K_s} + \frac{\phi}{K_f} \right]^{-1}$, with K_s , K_m and K_f the solid grains, dry matrix and saturant fluid bulk moduli; μ is the shear modulus, η is the fluid viscosity, κ is the permeability, ϕ the porosity, ω the frequency and i the imaginary unit.

Gelinsky and Shapiro (1997) determined the relaxed and un-relaxed stiffnesses of the equivalent poro-viscoelastic medium to such periodic sequences, while Krzikalla and Müller (2011) combined the two previous models, i.e., they computed p_{33} as in Eq.(3) and obtained the other five stiffnesses of the equivalent TIV medium as,

$$p_{ij}(\omega) = c_{ij} + \left(\frac{c_{ij} - c_{ij}^r}{c_{33} - c_{33}^r} \right) [p_{33}(\omega) - c_{33}], \quad (5)$$

where c_{ij}^r are the relaxed stiffnesses, computed as shown in the Appendix (Gelinsky and Shapiro, 1997). The main assumption in Eq. (5) is that the fluid-flow direction is perpendicular to the layering so that the relaxation behavior is described by a single stiffness, $p_{33}(\omega)$. Thus the theory is not valid when the layers are heterogeneous.

Velocity and quality factor of the qP, qS and SH waves for the equivalent anisotropic medium were computed from the complex velocities (see Carcione et al. (2005)).

RESULTS

Data

A dry core from the Vaca Muerta Formation is the source of the measured data, which consist of rock mineralogy and phase velocities, vp_{11} , vp_{33} , vp_{55} and vp_{66} of the core at 3100 m depth. This core corresponds to the window of maximum oil generation in the formation; its location is marked with a red rectangle in Figure 1.

The objective of this study is to verify that, by knowing the mineralogy and applying theoretical rock physics models, we can obtain an accurate estimate of the elastic tensor coefficients p_{ij} .

The numerical experiments consider an alternating periodic sequence of 1 mm thickness. Each period consists of eighty layers, seventy nine layers of Material 1 and one layer of Material 2.

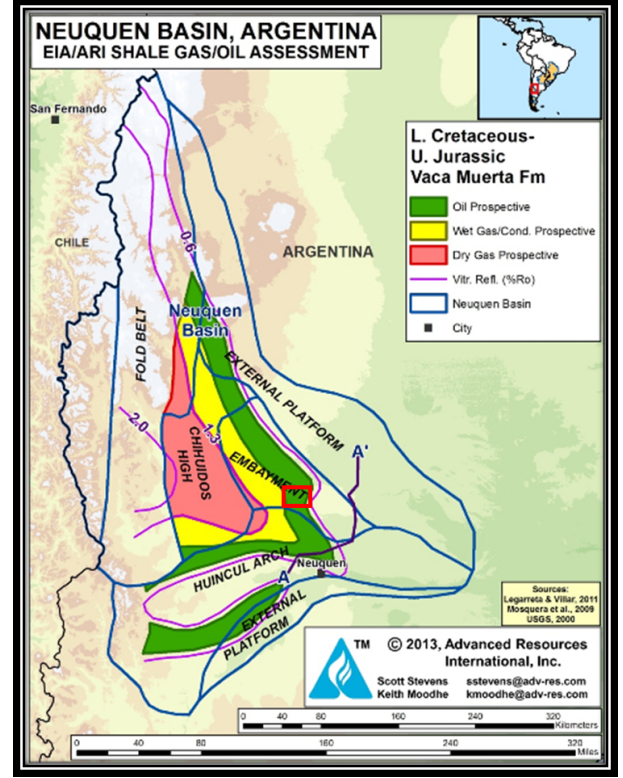


Figure 1: Location of the core area, marked with a red rectangle. The green region corresponds to the oil-generating window in the Vaca Muerta formation.

Material 1 is composed of seven minerals, including 23 % kerogen, 37.27 % Clay, 14.61 % Quartz, 10.68 % Calcite, 2.57 % Plagioclase, 2.37 % Dolomite and 3.5 % Pyrite. Using the solid grains density, bulk and shear moduli of each mineral and a generalized Krief model (see Carcione et al, 2005), we obtained the values K_s , K_m , μ_m for the dry core as shown in Table 1. We also computed the average density of Material 1. Besides, the single layer of Material 2 consists of dry kerogen. Its properties can be seen in Table 1. Both materials have 6 % porosity and $2.75 \cdot 10^{18} \text{ m}^2$ permeability.

Table 1. Properties of Materials

Property	Material 1 (Composite)	Material 2 (kerogen)
K_s (GPa)	34.34	7.0
K_m (GPa)	29.19	1.29
μ_m (GPa)	15.69	0.36
ρ (kg/m^3)	2487	1400

Computed VTI phase velocities using the dry-core data

We compute the numerical stiffness coefficients p_{ij} applying the methodology described in section "Mesoscopic-flow attenuation theory for VTI media" and the data of Table 1. We consider a 1 mm thickness periodic sequence, each period having seventy nine layers of Material 1 and one layer of Material 2. The mesh size is $1.25 \cdot 10^{-5} \text{ mm}$, then the sizes of layers 1 and 2 are $9.875 \cdot 10^{-4} \text{ mm}$ and $1.25 \cdot 10^{-5} \text{ mm}$, respectively. Since

From Mineralogy to Mechanical Properties using core data and rock physics for stiffness estimation in VMF

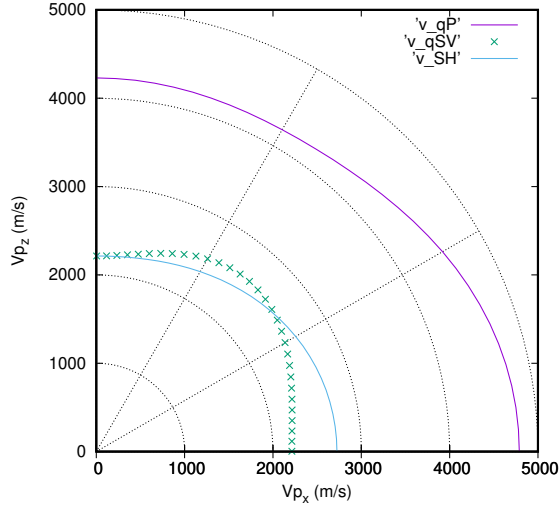


Figure 2: Polar representation of phase velocities of qP, qSV and SH waves at 1 MHz. The medium consists of a periodic sequence of seventy nine dry layers of the composite porous solid including kerogen as a mineral with 23 % proportion, and one dry kerogen layer.

the phase velocity data corresponds to a dry sample, the numerical experiment consider air as the saturating fluid. Table 2 summarizes the results of the VTI experiments.

Table 2. Phase velocities from the numerical experiments, the measured ones and error percentage. Frequency is 1 MHz

Phase velocity (m/s)	Computed	Measured	error (%)
v_{p11}	4538.29	4331	4.79
v_{p33}	4008.93	4217.47	4.96
v_{p55}	2098.69	2193.61	4.33
v_{p66}	2581.97	2464	4.79

In all computed velocities the error of less than 5% was obtained, which is considered a very good match since it is within the range of measurement errors. Hence we can then rely on the numerically estimated values of the stiffness coefficients p_{ij} shown in Table 3.

Table 3. Numerical p_{ij} values from the VTI experiments (Pa). Frequency is 1 MHz

$p_{11} = (47881607223.002250, 34039.066160)$
$p_{33} = (37362983980.381652, 223305.323451)$
$p_{55} = (10239564921.821903, 0.0)$
$p_{66} = (10239564921.827581, 0.0)$
$p_{13} = (13930827662.989664, 10086.232336)$

Figure 2 shows the polar representation of phase velocities of qP, qSV and SH waves of the dry core at 1 MHz. Anisotropy is clearly observed in the behavior of the velocities of the three wave modes.

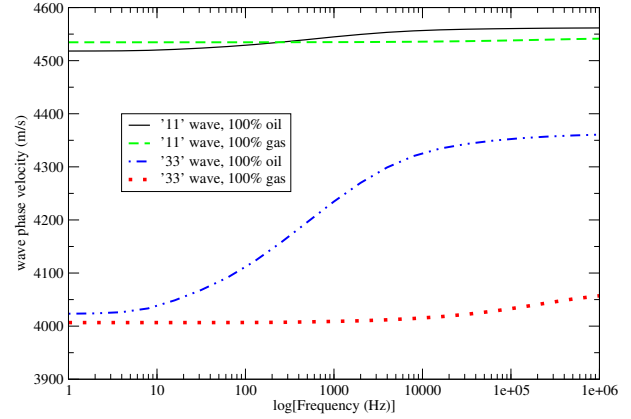


Figure 3: Wave phase velocity as function of frequency for '11' and '33' waves. The medium consists of a periodic sequence of seventy nine layers of the composite porous solid including 23 % of kerogen as a mineral and one kerogen layer. The pore space in both Materials is saturated with 100 % oil and 100 % gas.

Phase velocities and attenuation using using hydrocarbon saturated samples

This subsection considers the same sample of the previous experiment, but with the two periodic layers saturated by 100 % oil and 100 % gas. Figure 3 displays velocities of waves parallel ('11' waves) and normal ('33' waves) to the layering plane, as function of frequency. It may be observed that parallel velocities are higher than normal ones, but the kind of fluid affects more the normal velocities.

The corresponding attenuation factors $1000/Q_{11}$ and $1000/Q_{33}$ are displayed in Figure 4. Note that '33' waves exhibit more attenuation and the attenuation peaks are shifted to higher frequencies when the saturant fluid is gas.

CONCLUSIONS

We have presented a rock physics simulation-based methodology for estimating the stiffness tensor of a dry core sample from the Vaca Muerta formation in Neuquén, Argentina, using mineralogical characterization as input data. The proposed methodology was tested by comparing the numerical phase velocities with those measured in laboratory at 1 MHz, yielding excellent agreement. Furthermore, the procedure can be applied to study the influence of fluid saturation and different source frequencies at laboratory and field scales.

ACKNOWLEDGMENTS

We would like to thank Pluspetrol S.A. and Solaer Ingeniería S.A. for providing us with the measured data. This work was partially funded by the Universidad de Buenos Aires (UBA-CyT 20020190100236BA).

From Mineralogy to Mechanical Properties using core data and rock physics for stiffness estimation in VMF

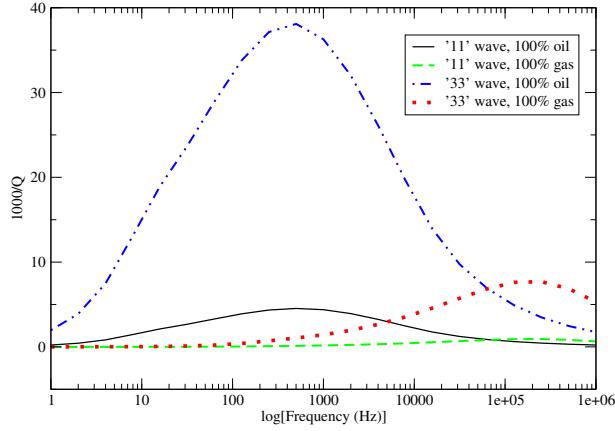


Figure 4: Attenuation factor $1000/Q$ as function of frequency for '11' and '33' waves. The medium consists of a periodic sequence of seventy nine layers of a composite porous solid including 23 % of kerogen as a mineral and one kerogen layer. The pore space in both Materials is saturated with 100 % oil and 100 % gas.

APPENDIX A

Following Gelinsky and Shapiro (1997), the relaxed stiffnesses are given by the expressions

$$\begin{aligned}
 c_{66}^r &= \langle \mu \rangle, \\
 c_{11}^r - 2c_{66}^r &= c_{12}^r = 2 \left\langle \frac{\lambda_m \mu}{E_m} \right\rangle + \left\langle \frac{\lambda_m}{E_m} \right\rangle^2 \left\langle \frac{1}{E_m} \right\rangle^{-1} \\
 &\quad + \frac{B_6^{*2}}{B_8^*}, \\
 c_{13}^r &= \left\langle \frac{\lambda_m}{E_m} \right\rangle \left\langle \frac{1}{E_m} \right\rangle^{-1} + \frac{B_6^* B_7^*}{B_8^*}, \\
 c_{33}^r &= \left[\left\langle \frac{1}{E_m} \right\rangle - \left\langle \frac{\alpha}{E_m} \right\rangle^2 \left\langle \frac{E_G}{M E_m} \right\rangle^{-1} \right]^{-1}, \\
 c_{55}^r &= \langle \mu^{-1} \rangle^{-1}, \\
 B_6^* &= -B_8^* \left(2 \left\langle \frac{\alpha \mu}{E_m} \right\rangle + \left\langle \frac{\alpha}{E_m} \right\rangle \left\langle \frac{\lambda_m}{E_m} \right\rangle \left\langle \frac{1}{E_m} \right\rangle^{-1} \right), \\
 B_7^* &= -B_8^* \left\langle \frac{\alpha}{E_m} \right\rangle \left\langle \frac{1}{E_m} \right\rangle^{-1}, \\
 B_8^* &= \left[\left\langle \frac{1}{M} \right\rangle + \left\langle \frac{\alpha^2}{E_m} \right\rangle - \left\langle \frac{\alpha}{E_m} \right\rangle^2 \left\langle \frac{1}{E_m} \right\rangle^{-1} \right]^{-1},
 \end{aligned} \tag{A-1}$$

where $\langle \cdot \rangle$ means weighted average between layers.

When there is no interlayer flow (unrelaxed regime), the coef-

ficients are,

$$\begin{aligned}
 c_{66} &= c_{66}^r, \\
 c_{11} - 2c_{66} &= c_{12} = 2 \left\langle \frac{(E_G - 2\mu)\mu}{E_G} \right\rangle + \left\langle \frac{E_G - 2\mu}{E_G} \right\rangle^2 \left\langle \frac{1}{E_G} \right\rangle^{-1}, \\
 c_{13} &= \left\langle \frac{E_G - 2\mu}{E_G} \right\rangle \left\langle \frac{1}{E_G} \right\rangle^{-1}, \\
 c_{33} &= \left\langle \frac{1}{E_G} \right\rangle^{-1}, \quad c_{55} = c_{55}^r.
 \end{aligned} \tag{A-2}$$

From Mineralogy to Mechanical Properties using core data and rock physics for stiffness estimation in VMF

REFERENCES

- Backus, G., 1962, Long-wave elastic anisotropy produced by horizontal layering: *J. Geophys. Res.*, **67**, 4427–4440.
- Carcione, J. M., H. H. B., J. E. Santos, and C. L. Ravazzoli, 2005, A constitutive equation and generalized gassmann modulus for multimineral porous media: *Geophysics*, **70**, N17–N26.
- Carcione, J. M., and S. Picotti, 2006, P-wave seismic attenuation by slow-wave diffusion: Effects of inhomogeneous rock properties: *Geophysics*, **71**, O1–O8.
- Gelinsky, S., and S. A. Shapiro, 1997, Poroelastic backus-averaging for anisotropic, layered fluid and gas saturated sediments: *Geophysics*, **62**, 1867–1878.
- Krzkikalla, F., and T. M. Müller, 2011, Anisotropic p-sv-wave dispersion and attenuation due to interlayer flow in thinly layered porous rocks: *Geophysics*, **76**, WA135–WA145.
- Sosa Massaro, A., M. Frydman, and S. Barredo, 2018, Estratigrafía mecánica de detalle aplicada al modelado geomecánico elástico anisotrópico en la formación vaca muerta: *Revista de la Asociación Geológica Argentina*, **75**, 258–268.
- Tsvankin, I., 2001, *Seismic signatures and analysis of reflection data in anisotropic media*: Elsevier.
- White, J. E., N. G. Mikhaylova, and F. M. Lyakhovitskiy, 1975, Low-frequency seismic waves in fluid-saturated layered rocks: *Izvestiya Academy of Sciences USSR, Physics of Solid Earth*, **10**, 654–659.